ChemComm

Accepted Manuscript

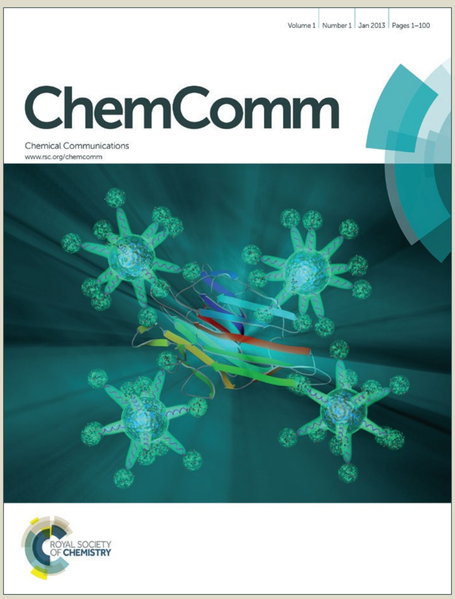

ROYAL SOCIETY OF CHEMISTRY

www.rsc.org/chemcomm

Journal Name

COMMUNICATION

CO_2 activation through silylimido and silylamido zirconium hydrides supported on N-donor chelating SBA15 surface ligand

Received 00th January 20xx,
Accepted 00th January 20xx

DOI: 10.1039/x0xx00000x

www.rsc.org/

Farhan Ahmad Pasha,[a]† Anissa Bendjeriou-Sedjerari,[a]† Edy Abou-Hamad,[a] Kuo-Wei Huang,[a] and Jean-Marie Basset[a*]

Density functional theory calculations and 2D ^{1}H-^{13}C HETCOR solid state NMR spectroscopy prove that CO_2 can probe, by its own reactivity, different types of N-donor surface ligands on SBA15-supported Zr^{IV} hydrides: [(≡Si-O-)(≡Si-N=)[Zr]H] and [(≡Si-NH-)(≡Si-X-)[Zr]H_2] (X= O or NH). Moreover, [(≡Si-O-)(≡Si-N=)[Zr]H] activates CO_2 more efficiently than the other complexes and leads to a carbimato Zr formate.

CO_2 activation and reduction for alternative energy source has received wide attention.[1-7] A variety of metal hydrides have been already tested for the CO_2 insertion and activation.[8-17] In certain cases, modelling studies have given important insight how these reactions occur and what factors are essential to determine the selectivity and efficiency.[18-23] Recently, amine-modified SBA15 surfaces with either silanol/silylamine, [(≡SiOH)(≡SiNH_2)] or bis-silylamine, [(≡SiNH_2)$_2$] pairs (named as [N,O] and [N,N], respectively) have demonstrated a potential role as new chelating ligands in surface organometallic chemistry (SOMC). Interestingly, their use as N-donor surface ligands allow the isolation of species defined as putative in molecular chemistry.[24-26] Thus, the design of π bond between the transition metal and the N-donor SBA15 surface ligands is achieved through the hydrogen treatment of a bipodal silylamido-silyloxo bis-neopentyl zirconium **1** (Scheme 1). This reaction was not observed with bipodal bis-silylamido bis-neopentyl zirconium **2**. As reported earlier, the formation of different hydride complexes **1a-c** and **2a-c** (Scheme 1) were confirmed by advance solid state NMR and FTIR spectroscopy.[25] However, the unambiguous identification of **1b**, whose homogenous counterpart has been reported to be only putative, was not achieved.[27, 28] Herein, we demonstrated a combined experimental and computation study utilizing CO_2 to support the formation of those zirconium hydride species supported on N-donor SBA15.

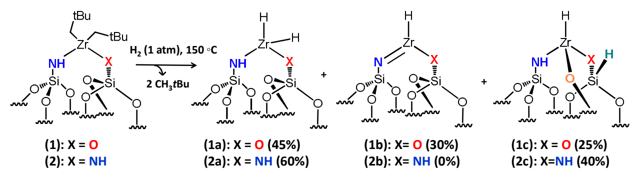

Scheme 1: Synthesis of Zr hydrides supported on [N,O] and [N,N] SBA15.[25, 26]

The reactivity of CO_2 on zirconium hydride supported on unmodified silica was studied first by our group.[29] The synthesis of either [(≡SiO)$_3$[Zr]H], tripodal zirconium monohydride or [(≡SiO)$_2$[Zr]H_2], bipodal zirconium bis-hydride were not possible due to surface heterogeneity resulting from heat treatment. The main product was the tripodal zirconium monohydride [(≡SiO)$_3$[Zr]H], (80%). The work was followed by a more recent computational study.[30] The main difference of the current work with all previous works is the presence of [N,O] and [N,N] isolated chelating pairs in close vicinity which allows the formation of a chelated metal with π bond between transition metal and the N-donors surface ligands (Scheme 1). The CO_2 insertion may take place on the zirconium bis-hydride, **1a** and **2a** as shown in scheme 2. In this case, the insertion of two molecules of CO_2 in two different Zr-H bonds is possible. The PES diagram (Fig.1) is drawn assuming energy of "naked" complex as 0.00 kcal.mol^{-1}. The coordination energy for the first CO_2 molecule is 1.9 and 2.8 kcal.mol^{-1} for **1a** (red profile) and **2a** (blue profile), respectively. The first insertion barrier is about 6.0 kcal.mol^{-1} for both, **1a** and **2a**.

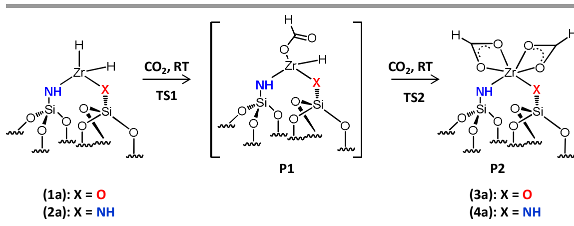

Scheme 2: CO_2 insertion into zirconium bis-hydride **1a** and **2a** yielding to zirconium bis-formate **3a** and **4a** respectively.

[a.] *KAUST Catalysis Research Center, King Abdullah University of Science and Technology, Thuwal 23955-6900, Saudi Arabia. Email: jeanmarie.basset@kaust.edu.sa*
† Authors have equal contributions.
Electronic Supplementary Information (ESI) available: [details of any supplementary information available should be included here]. See DOI: 10.1039/x0xx00000x

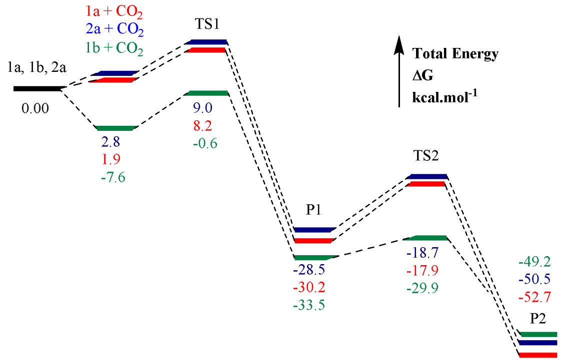

Fig-1: PES diagram for CO_2 insertion **1a** (red) and **2a** (blue) and **1b** (green). TS = Transition state.

However the products, P1 are stabilized with respect to the starting hydride complexes by a factor of 30.2 and 28.5 kcal.mol^{-1} for **1a** and **2a**, respectively. The insertion of the second CO_2 molecule to the remaining zirconium hydride is slightly energy consuming. The barrier is 12.3 and 9.8 kcal.mol^{-1} for **1a** and **2a**, respectively. The overall process is highly exergonic and the bis-formate, P2 adducts are 52.7 and 50.5 kcal.mol^{-1} more stable than the starting complexes, **1a** and **2a.** Furthermore, we have explored the CO_2 insertion possibilities to [(≡Si-O-)(≡Si-N=)[Zr]H] complex **1b** through the Zr-H and/or Zr=N bonds. Two pathways may occur (Fig. S1, see ESI). The green path shows a first CO_2 insertion into the Zr-H σ bond and a second into the Zr=N imido π bond while the blue path shows the insertion into Zr=N bond followed by an insertion into Zr-H bond. There was no dramatic difference between the two paths. At first the insertion of coordinated CO_2 into the Zr-H bond (R→P1) (TS1) barrier was 6.9 kcal.mol^{-1} (Fig.1) while the insertion of CO_2 into the Zr=N bond (R→P1') (TS1') barrier was 8.7 kcal.mol^{-1}. However the P1 and P1' stabilities exhibit significant difference, (P1= -33.5 and P1'= -20.6 kcal.mol^{-1}) with respect to the starting complex. Indeed, the green path is preferred and the first CO_2 insertion takes place at the Zr-H σ bond in **1b**. The coordination of the second molecule of CO_2 will further stabilize the overall system and its insertion barrier (P1→P2) (TS2) is 3.6 kcal.mol^{-1}. At the same time the insertion barrier of CO_2 to P1' (P1'→P2) (TS2') via blue path is found as 6.0 kcal.mol^{-1}. The difference between the two barriers P1→P2 and P1'→P2 is small but the P1→P2 pathway is preferred because of thermodynamic stability of P1 with respect to P1'.

Similarly, the CO_2 insertions into the other zirconium monohydrides (**1c** and **2c**) take place via the reaction described in scheme 3. The activation processes were analysed over potential energy surface. The CO_2 coordination energy ΔG for the tripodal zirconium monohydride [N,O,O] **1c** (red profile) and [N,N,O] **2c** (blue profile) is found as 4.7 and 3.6 kcal.mol^{-1}, respectively, including entropic corrections (Fig. 2A). The CO_2 insertion to Zr–H bonds occurs through a four-centered (TS) with a barrier of 10.1 and 9.4 kcal.mol^{-1} for **1c** and **2c**, respectively.

The tripodal [N,O,O] coordinated Zr-H (**1c** + CO_2, Fig. 2B) seems to be more electronegative as the distance of Zr-O bond is slightly lower, 2.34 Å than that of [N,N,O] supported Zr-H (**2c** + CO_2, Fig 2C), 2.39 Å. The overall CO_2 insertion process into Zr-H is an exergonic process (in terms of free energy). The CO_2 adduct for **1c** and **2c** was -28.0 and -27.6 kcal.mol^{-1}, respectively more stable than the starting material.

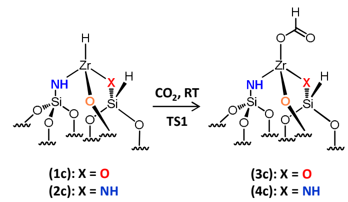

Scheme 3: CO_2 insertion into zirconium monohydride **1c** and **2c** leading to the zirconium monoformate **3c** and **4c,** respectively.

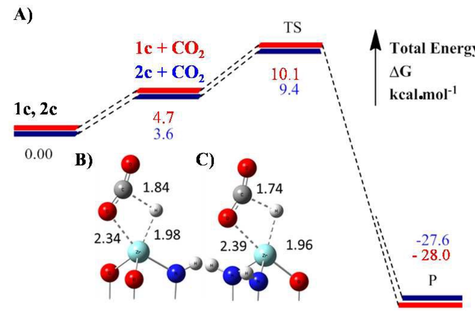

Fig-2: (A) PES diagram for CO_2 insertion over tripodal zirconium monohydride, **1c** (red) and **2c** (blue) and their respective first TS geometries (B) and (C).

A close look at the transition state geometries (Fig-S2, ESI) for CO_2 insertion at **1a** and **2a** indicates that, geometries are very similar for the complexes **1a** and **2a** but the interatomic distances between anchoring N and O of **1a** is 3.0 Å and bond (N-Zr-O) angle is 98 ° while in **2a** the anchoring N and N distance is 3.5 Å and bond (N-Zr-N) angle is 115 °. Moreover, the comparison of the insertion barrier of CO_2 into Zr-H σ bond in **1a** and **1b** (Fig. 1 and S1) indicates clearly that the presence of Zr=N bond facilitates the CO_2 insertion into Zr-H bond. The same conclusion arises by comparing the insertion barrier of Zr-H σ bond in case of 1c and 1b (Fig.2 and Fig.S1).

The natural bonding orbital (NBO) analysis was also performed for the reactant, TS and product involved in CO_2 insertion for different complexes. The zirconium is an 8-electron d^0-system. The charge transfer from ligand to metal as well as the positive charge density on the metal play important role for the CO_2 insertion. The Zr centre has a positive density along the reaction coordinates as presented in Table S1. Among **1a**, **2a** and **1b** for reactant "R", the highest positive density/least charge transfer is associated with **1b** which apparently facilitates the CO_2 insertion. Complexes **1c** and **2c** have only one CO_2 insertion possibility. Even though the positive density is high there is no significant effect in the TS on the positive density which remains the same as in the reactant. However in the case of **1b** there is a significant effect on the positive density at TS2 (from 1.89 to 2.17 e). In this way, the Δq for R to P2 are respectively 0.40, 0.44, 0.37, 0.26 and 0.27 for complexes **1a**, **2a**, **1b**, **1c** and **2c**. After charge analysis it is interesting to see via the molecular orbital diagram, how this charge transfer affects and what atomic orbitals are involved in the frontier orbitals of molecule. We have thus analysed the first transition states in the three most active cases (**1a**, **2a** and **1b**); the details are presented in Fig. 3. In case of **1a** the highest occupied molecular orbital (HOMO) of TS1 consists mainly of Zr-H bond, out of which the Zr contribution is 32% while the H

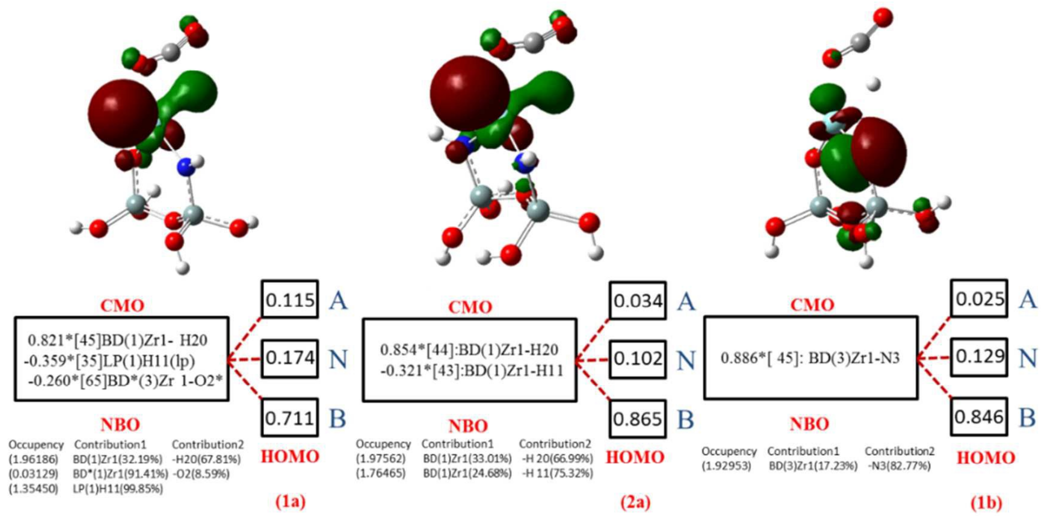

Fig. 3: The fractional constitution, partial distribution and contour of highest occupied molecular orbital (HOMO) diagram based on NBO analysis for **1a** (left), **2a** (middle) and **1b** (right).

contributing is 67.8%. The transferring H behaves like free radical hydrogen and 100% contributing to HOMO, at the same time minor contribution exhibited from antibonding (A) Zr-O orbital. The HOMO distribution for bonding (B), non-bonding (NB) and anti-bonding (A) is 0.71, 0.17 and 0.11 as mentioned in Fig. 3.

Similarly in case of **2a** the highest occupied molecular orbital (HOMO) mainly consists of both Zr-H bonds and H contribution is major while Zr contribution is minor. The HOMO distribution for bonding (B), non-bonding (NB) and anti-bonding (A) in **2a** is 0.86, 0.10 and 0.03. In the case of **1b** HOMO density is mainly centered on the Zr-N bond where Zr contribution is 17.2 % whereas the N contribution is 82.7%. The respective HOMO distribution for bonding, non-bonding and anti-bonding is 0.84, 0.12 and 0.02. Based on this observation it appears that the nitrogen modified SBA15 surface perturbs the electron density at the Zr metal centre. The Zr-imido system in **1b** should be most active for CO_2 coordination because this ligand leads to the lowest electron density at the metal center.

In order to confirm these theoretical calculations we performed experiments at room temperature and passed $^{13}CO_2$ over the materials displaying the different SBA15 supported zirconium hydrides complexes **1a, 1b, 1c** and **2a**, **2c** (Scheme 1). As previously described,[29, 30] zirconium hydride supported on silica reacts quickly with CO_2. Interestingly, not only zirconium hydride, but also the silylimido surface ligand **1b** reacts with $^{13}CO_2$, to yield as expected by modelling, a new [N,O] bound cyclic zirconium formate carbimato complex **3b** (Scheme 4) characterized by 2D ^{1}H-^{13}C HETCOR solid state NMR spectroscopy.

Upon $^{13}CO_2$ addition (200 Torr, 2h, at room temperature), zirconium hydrides complexes (grey solid) are instantaneously converted into their zirconium formates analogues (white off solid). This in agreement with the complete disappearance of the proton resonance at 10, 12 and 14 ppm assigned to the different zirconium hydrides (**1a**, **1b**, **1c** and **2a**, **2c**)[25] and the appearance of a new broad proton signal around 8 ppm in the ^{1}H MAS NMR spectra (Fig. S3-S4, ESI). This proton resonance is attributed to the proton of the formate zirconium complexes **3a**, **3b**, **3c** and **4a, 4c** (Scheme 2-4). The ^{13}C MAS experiments revealed more simple patterns: the spectrum of **3a, 3b** and **3c** exhibited four well-resolved signals at 180.7, 167.7, 161.2 and 55.5 ppm (Fig.4) while the spectrum of materials **4a** and **4c** shows only three resonances at 181.3, 169.4, and 56.6 (Fig. 5).

Furthermore, the 2D ^{13}C-^{1}H HETCOR spectrum of **3a, 3b** and **3c** shows a strong correlation between proton resonances at around 8 ppm in F2 and carbon resonances at 180.7, 167.7 and 161.2 in F1. The signals at 180.7 and 167.7 ppm correspond to the carbonyl group of the monoformate and bis(formate) zirconium, respectively.[29] As described in Scheme 4, **1b** contains both a zirconium hydride and a silylimido surface ligands. An imido metal complex, is also known to react swiftly with CO_2 to generate a carbimato metal complex.[31] So, upon the reaction with $^{13}CO_2$ a new N,O-bound carbimato zirconium-formate complex is generated. The chemical shift depicted at 161.2 ppm can be readily assigned to the carbon corresponding to the carbimato carbon in **3b**. As expected, the 2D ^{13}C-^{1}H HETCOR spectrum of **2a** and **2b** after reaction with $^{13}CO_2$ features only the two signals at 181 and 169 ppm assigned previously to zirconium mono and bis-formate, **4a** and **4c** respectively. The carbon peak at 55.5 ppm observed for all materials corresponds to a methoxy fragment. [29]

In summary, DFT calculations and experimental data successfully show that the insertion and the activation of CO_2 with amine-modified SBA15 supported zirconium hydrides is globally an easy process. CO_2 is highly reactive towards supported zirconium hydrides complexes and specifically with that containing a silylimido bond, [(≡Si-O-)(≡Si-N=)[Zr]H] **1b**. Indeed, in the case of complex **1b**, coordination of CO_2 results in the stabilisation of the adduct. The first CO_2 insertion into Zr-H bond is about 7 $kcal.mol^{-1}$ while the second CO_2 insertion into silylimido bond, N=Zr is about 3.6 kcal.mol^{-1}.

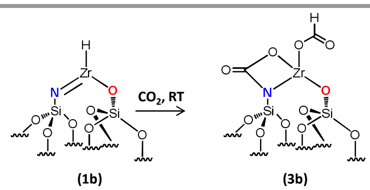

Scheme 4: CO_2 insertion into zirconium imido mono-hydride **1b** yields to the carbimato zirconium mono-formate **3b**.

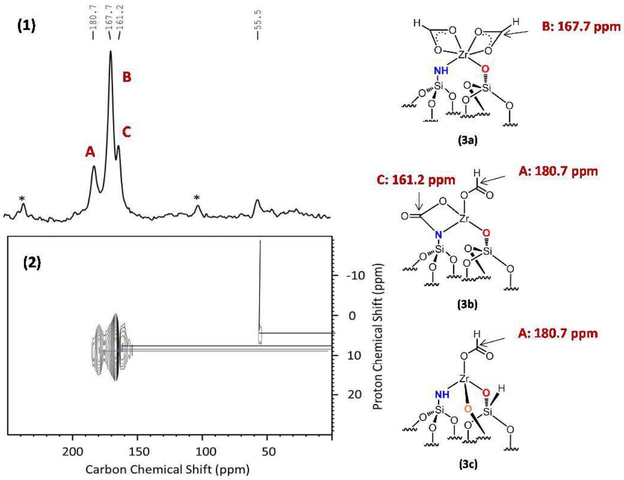

Fig.4 (1) ^{13}C CP-MAS NMR spectrum of **3a**, **3b** and **3c** and (2) 2D carbon-proton hetero nuclear dipolar correlation (HETCOR) spectrum of **3a**, **3b** and **3c.**

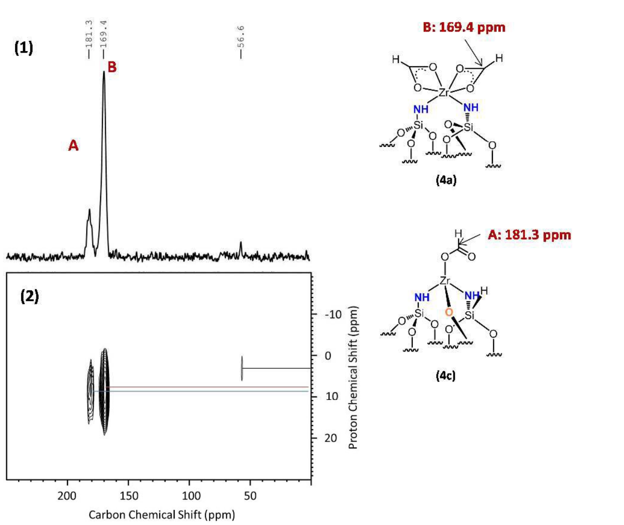

Fig-5. (1) ^{13}C CP-MAS NMR spectrum of **4a** and **4c** and (2) 2D carbon-proton hetero nuclear dipolar correlation (HETCOR) spectrum of **4a**, and **4c**

This publication is based upon work supported by the King Abdullah University of Science and Technology (KAUST) Office of Sponsored Research (OSR) under Award No CRG_R2_13_BASS_KAUST_1Notes and references

1. R. Angamuthu, P. Byers, M. Lutz, A. L. Spek and E. Bouwman, *Science*, 2010, **327**, 313-315.
2. C. D. Gomes, O. Jacquet, C. Villiers, P. Thuery, M. Ephritikhine and T. Cantat, *Angew. Chem. Int. Edit.*, 2012, **51**, 187-190.
3. Y. F. Jiang, O. Blacque, T. Fox and H. Berke, *J. Am. Chem. Soc.*, 2013, **135**, 7751-7760.
4. G. A. Olah, *Angew. Chem. Int. Edit.*, 2005, **44**, 2636-2639.
5. F. Huang, C. Zhang, J. Jiang, Z.-X. Wang and H. Guan, *Inorg. Chem.*, 2011, **50**, 3816-3825.
6. S. Chakraborty, J. Zhang, J. A. Krause and H. Guan, *J. Am. Chem. Soc.*, 2010, **132**, 8872-8873.
7. M. Wen, F. Huang, G. Lu and Z.-X. Wang, *Inorg. Chem.*, 2013, **52**, 12098-12107.
8. D. Walther, H. Schonberg, E. Dinjus and J. Sieler, *J. Organomet. Chem.*, 1987, **334**, 377-388.
9. D. Walther and V. Herzog, *Z. Chem.*, 1987, **27**, 373-374.
10. D. Walther, *Coordin. Chem. Rev.*, 1987, **79**, 135-174.
11. D. J. Darensbourg, A. Rokicki and M. Y. Darensbourg, *J. Am. Chem. Soc.*, 1981, **103**, 3223-3224.
12. D. J. Darensbourg and A. Rokicki, *Organometallics*, 1982, **1**, 1685-1693.
13. D. J. Darensbourg and A. Rokicki, *J. Am. Chem. Soc.*, 1982, **104**, 349-350.
14. Y. Jiang, O. Blacque, T. Fox and H. Berke, *J. Am. Chem. Soc.*, 2013, **135**, 7751-7760.
15. S. Kato, A. Borgschulte, D. Ferri, M. Bielmann, J.-C. Crivello, D. Wiedenmann, M. Parlinska-Wojtan, P. Rossbach, Y. Lu, A. Remhof and A. Zuttel, *Phys. Chem. Phys. Chem.*, 2012, **14**, 5518-5526.
16. J. Li and K. Yoshizawa, *Bull. Chem. Soc. Jpn.*, 2011, **84**, 1039-1048.
17. S. Chakraborty, P. Bhattacharya, H. Dai and H. Guan, *Acc. Chem. Res.*, 2015, **48**, 1995-2003.
18. B. P. Sullivan, C. M. Bolinger, D. Conrad, W. J. Vining and T. J. Meyer, *J. Chem. Soc. Chem. Comm.*, 1985, 1414-1415.
19. C. M. Bolinger, B. P. Sullivan, D. Conrad, J. A. Gilbert, N. Story and T. J. Meyer, *J. Chem. Soc. Chem. Comm.*, 1985, DOI: Doi 10.1039/C39850000796, 796-797.
20. C. M. Bolinger, N. Story, B. P. Sullivan and T. J. Meyer, *Inorg. Chem.*, 1988, **27**, 4582-4587.
21. M. R. M. Bruce, E. Megehee, B. P. Sullivan, H. Thorp, T. R. Otoole, A. Downard and T. J. Meyer, *Organometallics*, 1988, **7**, 238-240.
22. Y. Huang, S. Xu and V. S. Y. Lin, *Angew. Chem. Int. Ed.*, 2011, **50**, 661-664.
23. C. W. Machan, M. D. Sampson and C. P. Kubiak, *J. Am. Chem. Soc.*, 2015, **137**, 8564-8571.
24. A. Bendjeriou-Sedjerari, J. Pelletier, E. AbouHamad, L. Emsley and J.-M. Basset, *Chem. Comm.*, 2012.
25. A. Bendjeriou-Sedjerari, J. M. Azzi, E. Abou-Hamad, D. H. Anjum, F. A. Pasha, K.-W. Huang, L. Emsley and J.-M. Basset, *J. Am. Chem. Soc.*, 2013, **135**, 17943-17951.
26. F. A. Pasha, A. Bendjeriou-Sedjerari, K.-W. Huang and J.-M. Basset, *Organometallics*, 2014, **33**, 3320-3327.
27. C. P. Schaller, C. C. Cummins and P. T. Wolczanski, *J. Am. Chem. Soc.*, 1996, **118**, 591-611.
28. D. F. Schafer, P. T. Wolczanski and E. B. Lobkovsky, *Organometallics*, 2011, **30**, 6518-6538.
29. F. Rataboul, A. Baudouin, C. Thieuleux, L. Veyre, C. Copéret, J. Thivolle-Cazat, J.-M. Basset, A. Lesage and L. Emsley, *J. Am. Chem. Soc.*, 2004, **126**, 12541-12550.

30. M. P. Kalhor, R. Wischert, C. Coperet and H. Chermette, *New J. Chem.*, 2014, **38**, 3717-3721.
31. C. L. Boyd, E. Clot, A. E. Guiducci and P. Mountford, *Organometallics*, 2005, **24**, 2347-2367.